

Evaluation the effectiveness of an indirect solar dryer under Aswan governorate conditions

Mostafa O. Hassan^{a*}, Loai Nasrat^b, Wael A. Mahmoud^c and Taraby H.H.H.^a

^a *Department of Agricultural Engineering and Biosystems, Faculty of Agriculture and Natural Resources, Aswan University, Egypt.*

^b *Electrical Engineering Department, Faculty of Engineering, Aswan University, Aswan, Egypt.*

^c *Faculty of Agricultural Engineering, Al-Azhar University (Assiut Branch), Assiut, Egypt.*

Received: 4/6/2023

Accepted: 26/9/2023

© Unit of Environmental Studies and Development, Aswan University

Abstract:

This paper presents an evaluation of an indirect solar dryer consisting of a solar collector, trays located in the drying chamber, and an air outlet opening above the drying chamber. The solar collector consists of a Corrugated galvanized steel panel painted black and covered with sheets of transparent glass, 3 mm thick from the top, and with dimensions of 2400 x 1100 mm. The side walls of the solar collector are made of wood, and the insulation is thermal wool with a 50 mm thickness and are painted black from the outside. The drying room measures 1100 x 1200 mm, is made of wood, is thermally insulated from the inside, and contains a number of shelves. The solar dryer was tested with a load of henna leaves, it was exposed to solar radiation from 8:00 a.m. to 3:00 p.m. A leaves of henna drying test is used to evaluate solar dryers, with a maximum average temperature of 56.2 °C for the load test. 3000 g of henna leaves were used in the load test to gauge how well the solar dryer worked. For the solar drying test, 3000 g of henna leaves were dried from a starting moisture content of 74% W.b to a final moisture content of 8.4% in 7 hours of sunlight. The drying rate was calculated to be 306.7 g/h for the load test. The drying efficiency was calculated to be 19.5%. The average collector efficiency was also discovered to be 79.7% for the load test.

Keywords: Performance Evaluation, Drying, Solar Radiation, leaves of Henna.

1- Introduction

The biggest problem now facing humanity is energy. Nonrenewable and renewable energy sources are the two main categories (**Perlin, 1999**). Energy research has been rapidly progressing toward clean, sustainable, and renewable energy systems, such wind, geothermal, and solar energy technologies, over the last few decades. These devices were created for a number of uses, such as drying and heating (**Chang and Kim, 2001; Moumni et al., 2004; Battisti and Corrado, 2005**).

Corresponding author*: E-mail address: mostafaomar@agr.aswu.edu.eg

Egypt's solar atlas, published in 1991, shows that it has a technical solar-thermal electricity generating potential of 73.6 Peta watt hour, an annual direct normal energy density of 1970–3200 kWh/m², and 2900–3200 hours of sunshine (**Comsan,2010**).

Henna thrives in heavy, fertile clay soils that are completely drained. It thrives in soils with a pH range of 4.3 to 8.0 and an annual precipitation of 0.2 to 4.2 meters. Henna is exported in excess of 10,000 t annually. The top exporting nations are Pakistan, Iran, Sudan, India, and Egypt, while the top importing nations are the Middle East and North Africa, Western Europe, and North America. About 1000 t of henna herbs are exported from Sudan annually. The United States (500-600 t/year), France (250 t/year), Saudi Arabia (3000 t/year), and Great Britain (100 t/year) are the top four importers (**Rehmat et al.,2020**).

Although it is generally agreed that properly designed forced-convection (active) solar dryers are more selective and controllable than the natural-circulation (passive) types, the latter are clearly inappropriate for remote rural village farm application in the majority of developing countries due to the need for electricity or fossil-fuel driven fans and/or the use of auxiliary heating sources, which makes both their capital, maintenance, and operational costs prohibitive. The "ventilated greenhouse dryer" has the benefit of low cost and simplicity in both on-site construction and operation for large scale applications in rural areas (**Ekechukwu and Norton,1999**).

Drying is the process of removing moisture from a product, such as by lowering water activity, which can slow down the rate of deterioration and retain the quality. Agricultural products can be securely kept for several days if they are dried to eliminate the maximum amount of moisture while retaining their active ingredients. Additionally, the amount of free water in the meal is greatly reduced during this procedure, which results in a concentration of dry matter without compromising the food's tissue, wholesomeness, or outward appearance. This drying process involves the material's internal mass and heat transfers (**Lamidi et al., 2019**).

The literature may show a variety of solar dryer kinds or designs. In light of the ongoing advancements in solar dryer design, it should be developed to consistently update the classifications of solar dryers. Additionally, other methods may be used to group solar dryers. In fact, there are many different categories of solar dryers that have been published in the literature (**Chaudhari and Salve, 2014; Tiwari et al., 2016**). In this study, solar dryers are categorized based on the way air flows, how the sun heats the product, and the type of drying chamber Figure (1.1) demonstrates the many types of solar dryers.

Lawsonia inermis L., sometimes known as henna bushes, is a member of the Lythraceae family of plants and is a shrub with both decorative and medicinal uses. Henna is a perennial plant that may live for up to 10 years in the ground after being planted. The stem, which contains colorful components, has simple, leathery leaves on either side that become brown when the branches reach maturity. From the Babylonians and the Pharaohs employed the henna plant in their religious rites, it is regarded as one of the medicinal, aromatic, and cosmetic plants that man has known since the dawn of the earliest civilizations. It is a tropical plant that presumably originated in South America,

Iran, or India. Cultivation of the plant has since expanded to Australia, North Africa, and southwest Asia (Ghani et al., 2021).

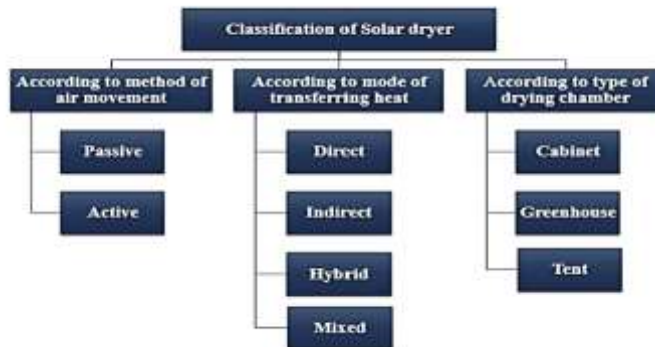


Figure (1): Classifications of solar dryers

Drying requires a lot of energy to do. The use of conventional and fossil fuel heating is expensive, inefficient for drying, and emits unwanted CO₂. Since it causes erosion and desertification, burning biomass is not a wise choice for heating. Drying typically involves the use of expensive energy sources like electricity or a mix of solar energy and another type of energy. Harnessing solar energy for heating agricultural goods is a low-cost solution in terms of both capital and operating expenditures (Akuffo et al., 2003). Solar energy is abundant in these remote areas of Egypt, where the amount of sunshine hours is around 3500 h/year (Ahmad and Schmid, 2002).

2. Materials and Methods

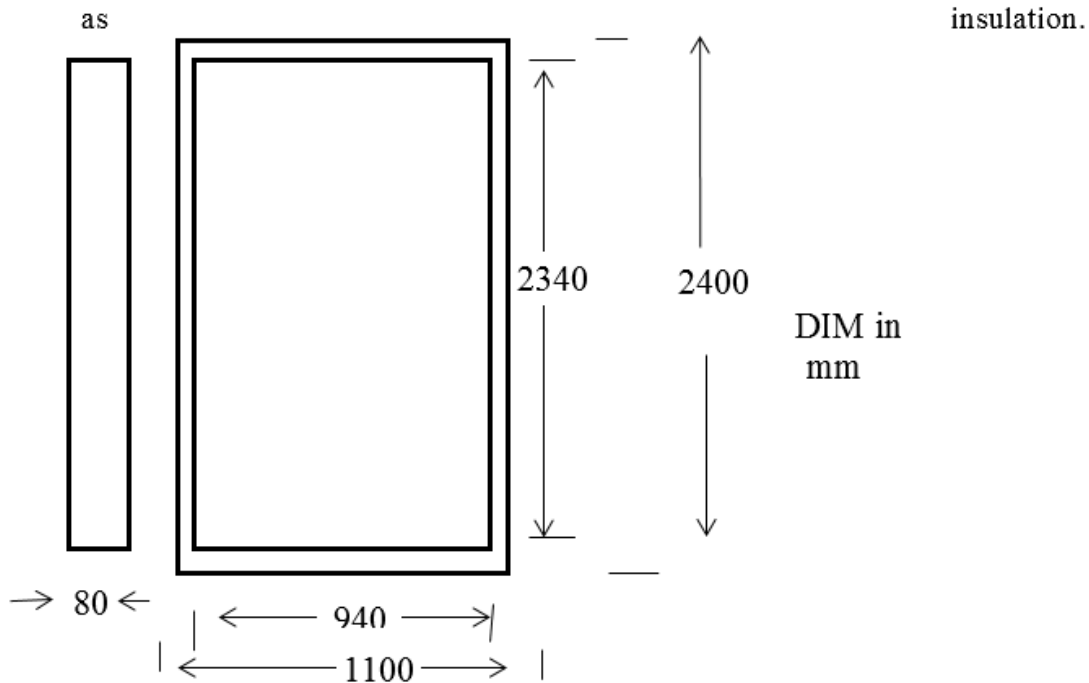
The performance assessment test was conducted using an indirect solar dryer. The indirect solar dryer was constructed in the workshop and tested on the campus of the College of Agriculture and Natural Resources at Aswan University, Egypt.

2.1. Components of the solar dryer

An indirect solar dryer consisting of a solar collector (SC), trays located in the drying chamber and exhaust fan.

2.1.1 Solar collector SC

The primary goal in building the solar collector was to use locally available materials to collect as much solar energy as possible at the lowest possible cost. SC performance evaluations were carried out in Egypt's governorate of Aswan. Latitude and longitude are 24.06° and 32.45°, respectively, with 14 hours of daylight and $I = 8.2 \text{ KWh/m}^2$ per day for a 24.06° solar declination angle. It is painted black to keep the heat inside and is thermally insulated with thermal wool that has a thickness of 50 mm. Three main parts make up the solar collector: The glass cover is 2400 mm long, 1100 mm wide, and 3 mm thick. The cover is fastened to a 100 mm-thick wooden frame. Corrugated galvanized steel black plate is used to create the absorber plate, the height between them was 10 cm. Thermal wool with a 50 mm thickness serves as shown figure (2).



Figure(2): solar collector “SC”.

2.1.1.1. Solar collector absorber plate

The air fluid receives the collected energy through the energy absorber plate. For effective heat absorption, the absorber plate was constructed from a Corrugated galvanized steel plate that was one millimeter thick and black-coated. 50° is the rib angle, and 5 cm is the top height.

2.1.1.2. Transparent glass cover.

In order to increase the temperature of the absorbent surface, the transparent glass plate absorbs the solar radiation that is directed towards it and allows it to enter the interior. The glass cover is 3 mm thick, 2400 mm long, and 1100 mm wide. Table (1) dimensions solar collector absorber plate and transparent glass cover.

Table (1) dimensions solar collector absorber plate and transparent glass cover.

Properties of cover material –glass	
Solar spectrum refractive index:	1.52
Transmittance:	0.89
Number of covers:	1
Cover-plate air spacing:	150 mm
solar collector glass cover dimensions length	2400mm
SC width	1100 mm
SC absorber area	2.256m ²
Properties of absorber plate	
Conductivity Iron:	60.50 W/m k ⁰
Thickness:	1 mm
Solar spectrum absorbance:	0.88

Properties of cover material –glass	
Long-wave emittance:	0.15
top height	50 mm
Ribbing angle	50°
solar collector absorber dimensions length	2400mm
SC width	940 mm
SC absorber area	2.256 mm

2.2. The drying chamber.

The drying chamber is made of wood with a thickness of 30 mm. It is thermally insulated by thermal wool with a thickness of 5 cm and painted black to trap the heat inside. The manufactured drying chamber can accommodate three or more trays and has an exhaust hole. The drying chamber has a length of 1100 mm, width of 0.65 m and height of 1200 mm. It is equipped with a two-piece door in the front. It is about 800 mm above the ground and carried on 4 legs.

2.3. Exhaust Fan/Ventilation Fan.

DC 12V exhaust fan, Material Plastic, with a diameter of 16 cm, a size of 150 mm, a capacity of 20 watts, and a frequency of 50 Hz. It is installed inside a circular hole; axial fan was used to draw hot air to the chamber Dryer.

Table (2) Ventilation Fan specifications

speed	Diameter	capacity	frequency	type	volt	Material
3	15 cm	20 watts	50 Hz	DC	12V	Plastic

2.4 Measuring instruments

2.4.1. Solar intensity device

System temperatures were recorded by the digital thermometer and the different measured point of a prototype using thermocouple type K, Ranged from -200 to 1250 °C, with accuracy of $\pm 1\%+3$. A Pyranometer model PSP was used to measure the solar radiation sensitive to 9 μV per W/m^2 . The Pyranometer readings were linear to $\pm 0.5\%$ in measurement ranged from 0 to 2800 W/m^2 .

2.4.2 Anemometer.

The anemometer apparatus is used for measuring air speed their specifications are shown in Table (3).

Table (3): Specifications of the anemometer.

Air Velocity	Range	Resolution	Accuracy
meters per sec	0 - 30m/s m/s	0.1 m/s	$\pm (3\% + 0.20 \text{ m/s})$
Air Flow	Range	Resolution	Area
cubic meters/min	0-9999 m^3/min	1	0 to 9.999 m^2
Air Temperature	Range	Resolution	Accuracy
	10 - 50 Deg.C	0.1 °F/c	4.0 °F (2.0 °C)

* Model UT363.

24.3 Electronic balance.

Model DT2000, Capacity(g) 2000, Readability(mg) 0.5, Linearity error(g) $\leq \pm 1$, Plan size 173x135mm, Dimension 230x178x66mm and Voltage AC 220V. The initial weight of the henna leaves to be dried was determined with an electronic balance Sensitive scale with three decimal digits before being inserted in the dryer. The weight was determined at every one-hour interval during the drying process.

2.4.4. Electronic circuit.

Table (4): Specifications of the Electronic circuit.

Q	Parameter	Specification	Job	Figures
1	Adriano Uno (ATmega328)	Operating Voltage 5V. DC Current for 3.3V Pin: 50 mA. Flash Memory: 32 KB. SRAM: 2 KB(ATmega328P)	Data storage	
5	Precision Digital Temperature and Humidity Sensor Module (DHT22))	3 to 5V power and I/O. 2.5mA max current use during conversion (while requesting data). Good for 0-100% humidity readings with 2-5% accuracy. Good for -40 to 25°C temperature readings $\pm 0.5^\circ\text{C}$ accuracy. 0.5Hz sampling rate.	A digital temperature and humidity sensor.	
1	Digital Temperature Sensor Module (DS18B20)	Unique 1-Wire interface requires only one port pin for communication. Each device has a unique 64-bit serial code stored in an onboard ROM. Can be powered from data line. Power supply range is 3.0V to	provides 9-bit to 12-bit temperature measurements and has an alarm function with on volatile user-programmable upper and lower trigger points.	

Q	Parameter	Specification	Job	Figures
		5.5V. Measures temperatures from -55°C to $+125^{\circ}\text{C}$. Thermometer resolution is user-selectable from 9 to 12 bits. User-definable nonvolatile (NV) alarm settings with Alarm search command. identifies devices whose temperature is outside of programmed limits.		

A device for measuring temperature and humidity is shown in the following figure (3):

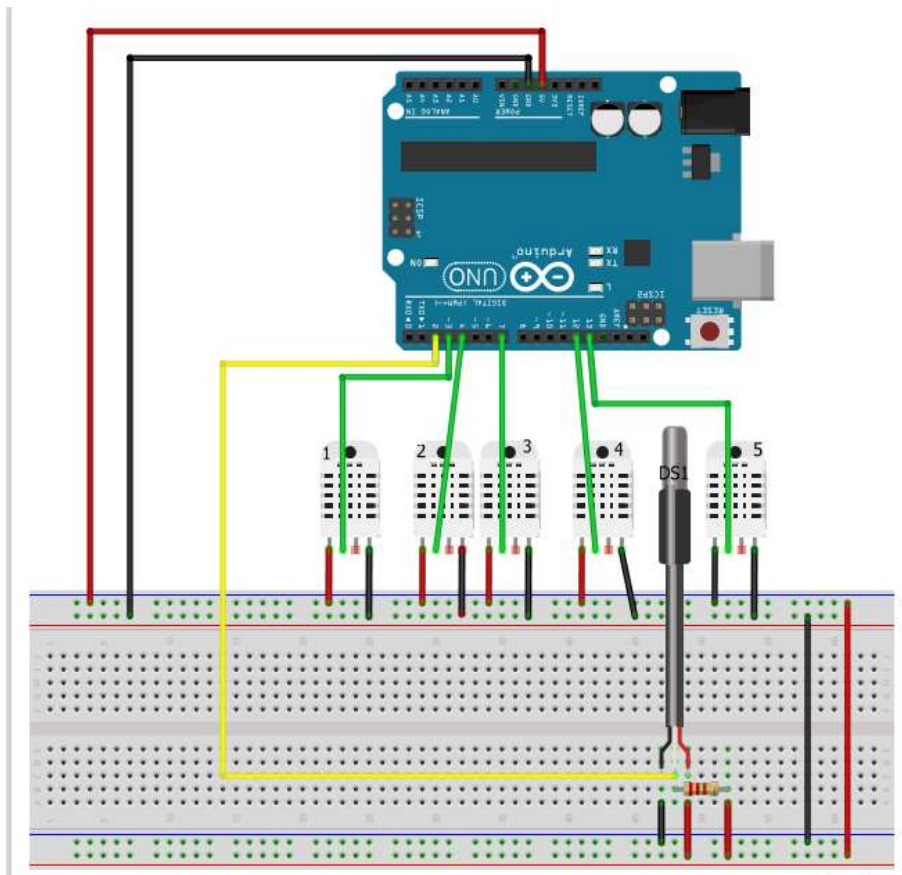


Figure (3): The circuit diagram

2.5. Performance evaluation of the solar dryer:

2.5.1 Solar collector efficiency

The solar collector was built on the presumption that it operates in a steady state, so the system analysis techniques described here can be used to use the thermal performance analysis to maximize system efficiency by **Duffie and Beckman (1991)**; **Kalogirou (2004)**; and **ASHREA (2005)** as follows:

$$\eta_{sc} = \frac{Q_u}{AI} \dots\dots\dots 1$$

Where; I is the solar radiation flux incident on the tilted surface of the SC W/m^2 , Q_u is the useful energy gain per time a solar collector "W".

$$Q_i = I.(\tau\alpha).A \dots\dots\dots 2$$

where Q_i is the absorbed solar energy, and A is the surface area of collector (m^2), τ is the transmittance of the SC covers, and α is the absorptance of the SC plate.

Overall heat transfer coefficient (**Awady, 1999**).

$$Q_o = UA(T_a - T_m) \dots\dots\dots 3$$

$$Q_u = Q_i - Q_o = I(\tau\alpha)A - UA(T_a - T_m)$$

$$Q_u = mC_p(T_h - T_c) \dots\dots\dots 4$$

where Q_i is the collector heat input "W", Q_o is the solar collector overall heat losses "W", m is the fluid mass flow rate (Kg/s), T_c is the temperature of cold air "°K", T_h is the temperature of hot air "°K", T_a is the SC average temperature "°K", T_m is the temperature of ambient still air "°K", and c_p is the air fluid heat capacity "kJ/kg °K".

2.5.1.1 solar collector thermal losses

Because of the various layers and components, each of which has a different set of thermal characteristics, it is challenging to measure the average solar collector temperature. as shown in figure (4).

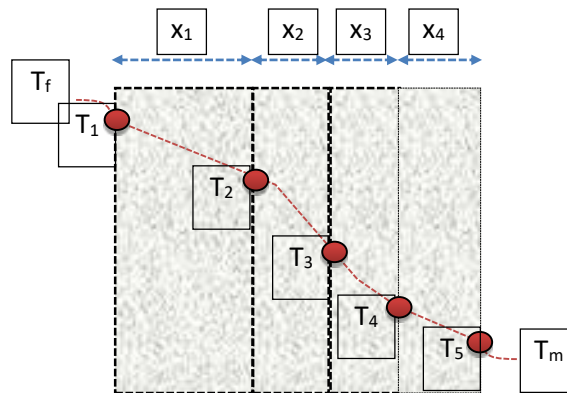


Figure 4: Heat transfer through layers of air, wood, glass wool and absorber plate.

$$R = \sum \frac{1}{UA} = \frac{1}{A_1 h_a} + \frac{X_1}{A_1 K_1} + \dots + \frac{X_n}{A_n K_n} + \frac{1}{A_n h_b} \dots\dots\dots 6$$

$$R = R_a + R_b + R_1 + R_2 + R_n \dots\dots\dots 7$$

$$R_{overall} = R_{glass\ wool} + R_{wood} \dots\dots\dots 8$$

$$U = \frac{1}{AR_{overall}} \dots \dots \dots 9$$

where **R** is the thermal resistance of insulation “°K/W”, **R₁** is the thermal resistance of inner layer of insulation “°K/W”, **R₂** is the thermal resistance of second layer of insulation “°K/W”, **R_n** is the thermal resistance of nth layer of insulation “°K/W”, **R_s** is the thermal resistance of outer surface of insulation “°K/W”, **h_b** is the surface coefficient of outer surface “W/m² °K”, **h_a** is the surface coefficient of inner surface “W/m² °K”, **k₁** is the thermal conductivity of inner layer of insulation “W/m °K”, **k₂** is the thermal conductivity of second layer of insulation “W/m °K”, and **k_n** is the thermal conductivity of nth layer of insulation “W/m °K”.

According to earlier equations, a wooden frame and glass-wool layers were used to cover the collector's back and sides in order to reduce heat losses from the FPC. The sum of the values for the conductivity of air, wood, glass wool, and absorber layers will determine the heat transfer's overall thermal conductivity (Awady, 1999).

2.5.2 Drying efficiency.

The ratio of energy used to heat the sample and evaporate its moisture to the total energy consumed is known as drying efficiency. This gauges the dryer's overall efficacy. (Forson et al., 2007; Drew, 2011 quoted from Brenndorfer et al, 1987).

$$\eta_d = \frac{M_w L}{I_T A_T t_d} \dots \dots \dots (10)$$

Where;

M_w = Mass of moisture removed by dryer (kg)

A_T = total area of collectors (m²)

I_T = Average solar insolation (W/m²)

L = Latent heat of evaporation of water (kJ/kg)

T_d = Overall drying time, (seconds)

2.5.3 Average drying rate.

The mass of moisture extracted by the drier, **M_w**, and drying time are used to calculate the average drying rate, **M_{dr}**, the amount of moisture that was taken out of the meal over the course of drying was given by (Tonui et al., 2014).

$$M_{dr} = \frac{M_w}{t_d} \dots \dots \dots (11)$$

Where,

M_{dr} = Average drying rate (kg/h)

M_w = Mass of moisture removed by dryer (kg)

T_d = Overall drying time (h)

2.5.4 Moisture content.

The amount of water in the produce is its moisture content. There are two methods for calculating the moisture content of produce: on a wet basis and on a dry basis, the amount of moisture in a material's original mass can be represented on a wet basis and expressed According to (Mohanraj and Chandrasekar, 2009).

On wet basis

$$M_{wb} = \frac{(M_i - M_f)}{M_f} \times 100 \dots\dots\dots (12)$$

On dry basis, moisture

$$M_{db} = \frac{(M_i - M_f)}{M_f} \times 100 \dots\dots\dots (13)$$

Where,

M_{wb} = moisture content on wet basis (%)

M_{db} = moisture content on dry basis (%)

m_i = Initial mass of the product before drying (kg)

m_f = Final mass of the product after drying (kg)

2.5.4 Moisture gain or loss.

This is the percentage increase or decrease in moisture during the night period. A negative value indicates further moisture loss while a positive value indicates moisture gain (Mohanraj and Chandrasekar, 2009). It can be calculated as;

$$M_n = \frac{M_{sr} - M_{ss}}{M_i} \dots\dots\dots (14)$$

Where;

M_{sr} = Mass at sunrise (kg)

M_{ss} = Mass at sunset (kg)

M_i = Initial mass of sample (kg)

2.6. Henna.

Lawsonia inermis L., sometimes known as henna bushes, is a member of the Lythraceae family of plants, annual or perennial, with a lifespan of about three years and may extend to ten, evergreen, abundantly branching, up to three meters long, and has roots and a red stake. henna was obtained from one of the local fields in Aswan. Its stem has many branches and lateral branches, and it is green in color. The shrub's height ranged from 2 to 3 meters, and the flower color was Miniata with purple flowers. Leaves are dark oval, 1.5-5 cm long, and 0.5-2 cm wide. Henna leaves contain different glycoside substances, the most important of which is the main substance known as (Lawson) and its chemical molecule of the type 2-hydroxy-1,4-naphthoquinone or 1,4-naphthoquinone. This substance is responsible for the biological effect in medicine as well as the red dye.

Henna consists of the following compounds: Dyes of type 41-naphthoquinone, including 1% Lawson (2-hydroxy-41-naphthoquinone), hydroxylated naphthalene derivatives such as 4-glucosyl and oxy-21-dihydroxy, coumarine, xanthone, flavonoids, 5-10% tannin, gallic acid, and a

low amount of steroid like sitosterol The flowers contain a volatile oil that has a sweet and strong smell, and its most important constituents are phobita ionones (A, B, and Ionone). The amount of active substances, especially lawson (which is the colouring matter), increases in henna leaves as the plant grows older, and young leaves contain small amounts of these substances compared to their aged counterparts. Besides that, they contain gallic acid and tannins in a ratio of 5–10 And sugary and resinous materials, at a rate of about 1%.

2.7 Experimental Procedures and Dryer Evaluation.

Fresh leaves of henna were obtained from one of the local fields in Aswan. The extraneous elements, such as weeds and damaged or discolored plants, and the initial moisture content of the henna leaves were determined by oven drying. The test was conducted on September 13, 2022. Relative humidity, the temperature, the initial and final mass of the henna leaves, and the speed of the wind were measured at various points during the experiment.

2.7.1 Load test.

Under the solar drying test, 3000 g of henna leaves were used for the test. Each tray was covered in a single layer of 1000g henna leaves. Additionally, the dryer's evaluation criteria were noted. The original moisture content of henna leaves was determined via oven drying, and the average value was 74%wb. The weight of the henna leaves spread out on each tray was then calculated using the formula: [Tray + henna leaves] - Tray = henna leaf weight. Trays containing the henna leaves were placed in the drying chamber. Based on the established initial moisture content, the decrease in weight of the henna leaves was measured and used to assess the moisture loss of the leaves during the drying process. Wet basis calculations were used to determine the moisture content at each point during the drying process. The henna leaves were dried further until there was no discernible loss of weight or moisture. Based on the drying rate, drying efficiency, and dryer's performance. Temperature and humidity are measured through a humidity and temperature sensor.

3. Results and discussion.

3.1. Test.

The solar drying test was conducted on September 13, 2022, using the solar dryer to dry the henna leaves. In this test, 3000 g of henna leaves in the form of two layers —1000 g in each tray—were dried over the course of nearly 7 daylight hours, going from a moisture content of 74.0% wb to a moisture content of 8.4% wb. A safe moisture content for storage is less than 10% (Sengar et al., 2018).

3.1. Variation of Temperature with time.

Where the Temperatures with time were recorded, represented graphically as in Fig (5).

The plate of collector attained a maximum temperature of 70 °C, tray 1 in the drying chamber recorded a temperature of 56.2 °C, and the ambient's average temperature was 42.21 °C at 14 h. The ambient temperature and the dryer's average temperature were 37.2 and 43.84 °C, respectively. A temperature increases of 5.01 °C above ambient resulted from this. The collector attained a minimum temperature of 55 °C, tray 3's drying chamber recorded 39.5 °C, and the

outside air temperature was measured at 28.08 °C at 8:00 a.m. It is also noted that the temperatures on the first shelf are higher than on the second and third shelves, and on the second shelf, they are higher than on the third shelf.

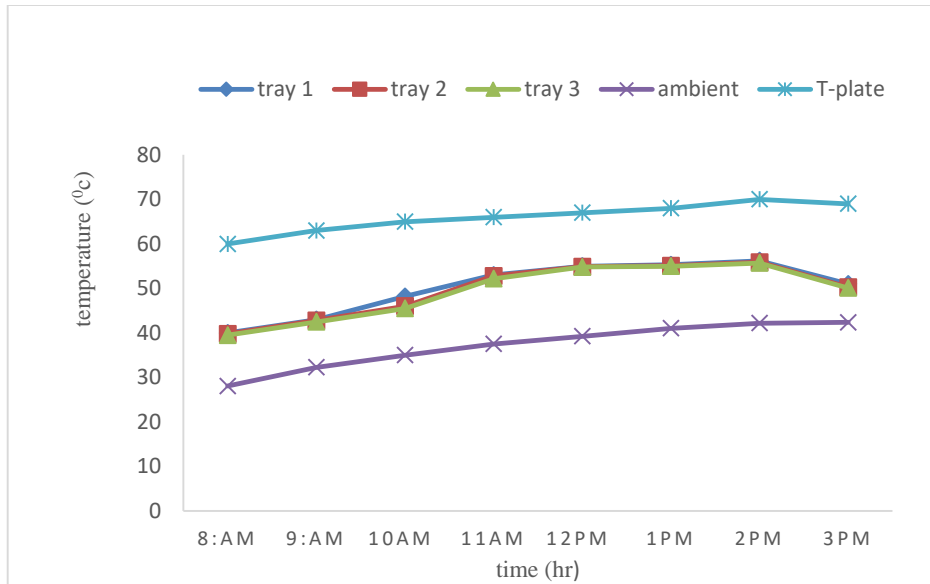


Figure (5). Variation of Temperature with time.

3.2. Variation of Moisture Content with time.

Where the Moisture Content with time were recorded, represented graphically as in Fig (6). The experiment began with a moisture content of 74.0% w.b and ended with a moisture content of 8.5% w.b in less than seven sunshine hours.

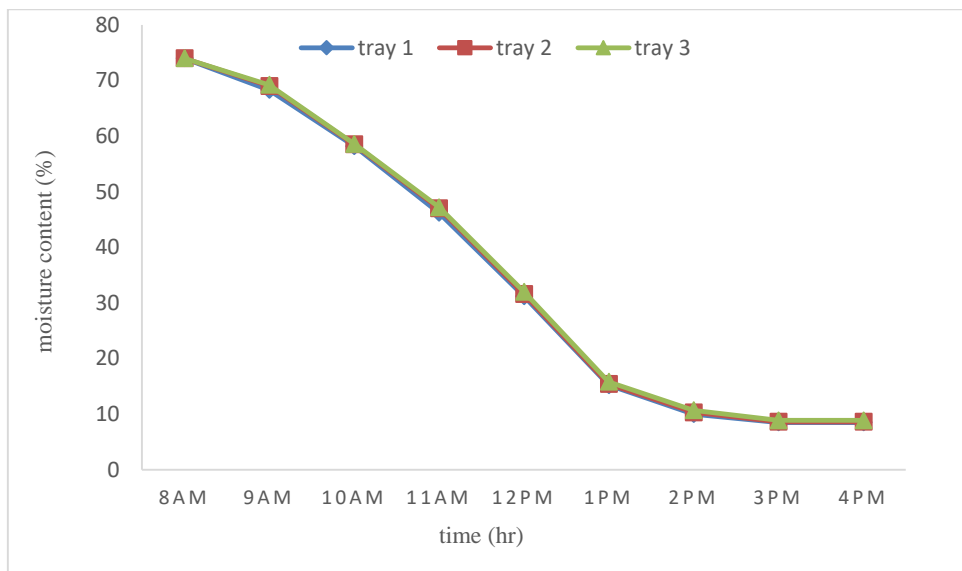


Figure (6). Variation of Moisture Content with time.

As observed in the graph, tray 1's sample lost water more quickly than trays 2 and 3's samples did. It was noted that the moisture content steadily decreased over time after starting out strongly. The correlation between drying rate and time-varying moisture content. the drying rate gradually decreased from its initial high level as the moisture content decreased (Sengar et al., 2018).

3.3. Variation of relative humidity with time.

Where the relative humidity with time were recorded, represented graphically as in Fig (7).

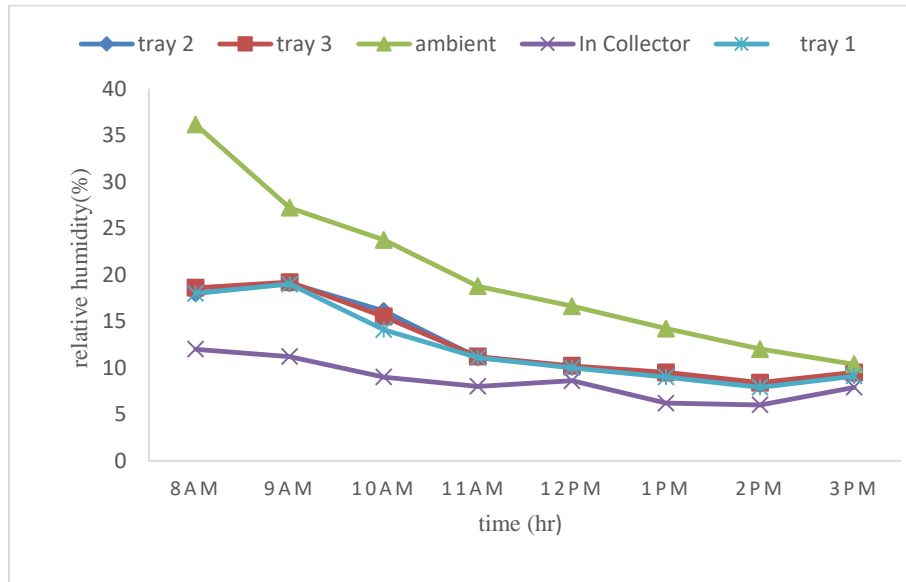


Figure (7). Variation of relative humidity with time.

Relative humidity vs time was plotted on the graph at three sections, at collector, ambient air and in chamber of dryer from 8:00 a.m. to 3:00 P.M. at one-hour interval. Figure (7) shows at first, it appeared that the relative humidity was nearly the same throughout. The relative humidity started to drop as the air heated up in the solar collector, and it was typically around 8.6%. At 8:00 a.m., the relative humidity at the chamber outlet started to rise as a result of the hot air from the collector entering the drying chamber evaporating moisture from the henna leaves. The relative humidity starts to fall as the henna leaves start to dry, which means that the rate of evaporation is slowing down with time. It is also noted that the relative humidity in the third shelf is higher than in the first and second, and in the second shelf is higher than in the first shelf.

Thermal performance analysis of the solar collector system

1. Load

Table 5. Thermal performance analysis of the solar collector system.

Time	Solar energy available	Absorbed solar energy	Useful heaty W	Solar collector losses w
8:00	1083.74	848.77	800.28	48.49
9:00	1633.2	1279.12	1183	96.12
10:00	2058.16	1611.17	1477	134.17
11:00	2326	1821.7	1364	457.7
12:00	2417.47	1893.36	1595	298.9
13:00	2327.077	1822.56	1410	412.56

Time	Solar energy available	Absorbed solar energy	Useful heaty W	Solar collector losses w
14:00	2057.9	1611.74	1356	255.74
15.00	1633.2	1279.12	1085.3	193.82

As shown (8).

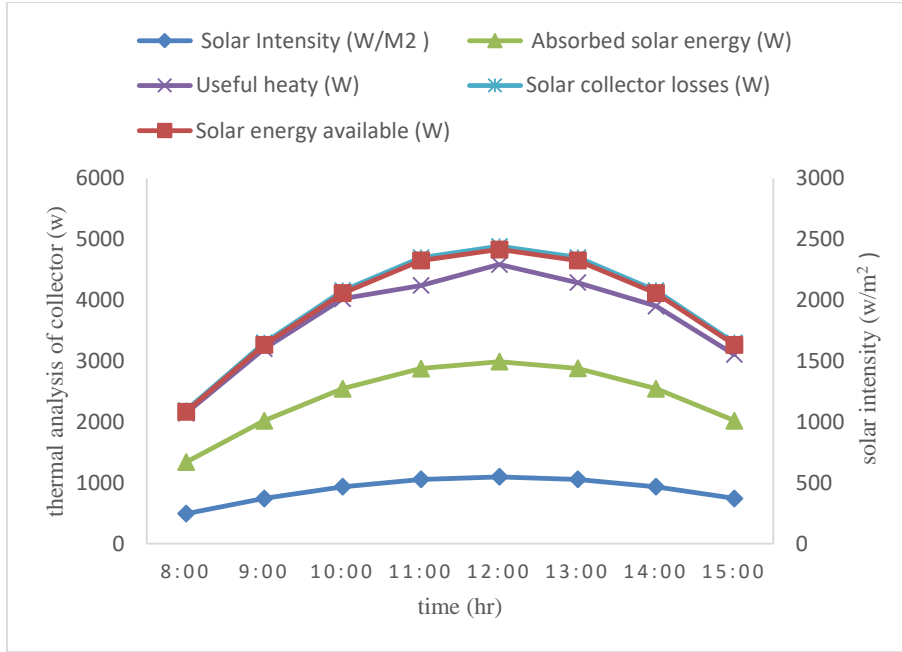


Fig.(8): The absorbed solar energy, Solar energy available, heat losses, collection useful heat for air as affected by time.

2.Noload

Table 6. Thermal Performance Analysis of the Solar Collector System.

Time	Solar energy available	Absorbed solar energy	Useful heat K	Solar collector losses
8:00	1096.3	858.62	769.5	89.12
9:00	1638.7	1283.4	900	383
10:00	2058.8	1612.45	1200	412
11:00	2324.97	1820.9	1200	620
12:00	2415.16	1891.55	1300	590
13:00	2324.97	1820.9	1698.4	122.5
14:00	2058.8	1612.45	1307.5	304
15.00	1638.7	1283.4	960	323.8

As shown (9).

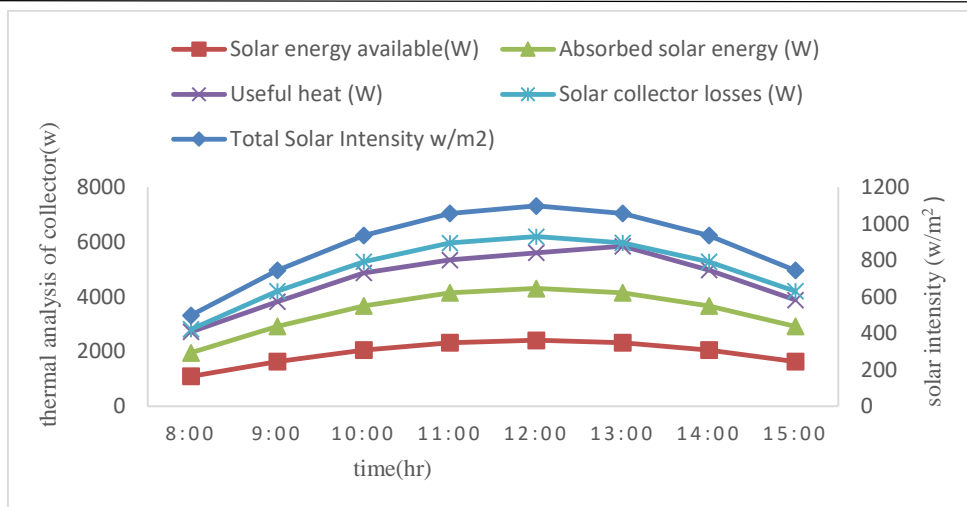


Fig.(9): The absorbed solar energy, Solar energy available, heat losses, collection useful heat for air as affected by time.

3. 3 Drying efficiency.

The drying efficiency of the dryer for the load test was evaluated at 19.5% for solar drying. Given that the efficiency of the collector is far better than that of the dryer, this solar collector could dry more leaves of henna in less time. The greater the loading density of the dryer, the higher its efficiency. This agrees with (Musembi et al., 2016).

In the case of favorable conditions during the load test of average temperature, relative humidity, solar radiation, and flow rate within 7 hours, the maximum efficiency of the dryer is equivalent to the efficiency of the solar collector, which is 79.7 %.

3.4. The effect of dryer efficiency on Lawsone pigment.

Lawson chemical present in the aqueous extract of henna leaves was tested using the TLC technique to determine the relative mobility (R_f) value. The R_f value of the Lawson compound is 0.4,

Which is identical to the standard value. This indicates that the compound is relatively well bound to, or interacts with, the adsorbent, providing further ability to note differences between the behavior of the target compound and other compounds. This is consistent with Simon et al. (1984) If the R_f value is between 0.5 and 0.2, this represents that the compound is relatively well bound or interacts with the adsorbent, providing further ability to note differences between the behavior of the target compound and other compounds.

It was discovered that the degree of colour of the compound Lawson is close to the degree of colour of the standard compound Lawson. This is proof of the excellent quality and substantial amount of Lawson compound contained in the aqueous extract of dried henna leaves. Lawson is the red orange hue and the primary colouring agent in henna, which is a reddish-orange molecule (2-hydroxy-1,4 naphtha quinone) that makes up 1–3% of the dry mass of dried leaves (Simon et al., 1984).



Figure (10). TLC for test.

4. Conclusion.

During the load test, leaves of henna with an average initial moisture content of 74.0% wb were dried to an average moisture content 8.4% wb within 7 hours, depending on the loading density of the product incorporating the lowest moisture content value. The performance of the dryer was evaluated in terms of its efficiency and drying rate. Results obtained from the test showed the collector efficiency for the load test was 80.5 percent. Moreover, the drying efficiency for the load test was 19.5%. The drying rate was 306.7 g/h for the load test, and the solar radiation was 800 w/ m². The maximum efficiency of the dryer is equivalent to the efficiency of the solar collector, which is 79.7%, and accordingly. According to the tests, it was observed that the efficiency of the collector is much higher than the efficiency of the dryer, so this solar collector can dry more. It was possible to increase the efficiency of the dryer if the capacity was larger.

REFERENCES

Ahmad, G. E. and Schmid, J. (2002): Feasibility study of brackish water desalination in the Egyptian deserts and rural regions using PV systems. *Energy Conversion and Management*, 43(18), 2641-2649.

ASHRAE, (2005): Handbook of Fundamentals “American Society of Heating, Refrigerating and Air Conditioning Engineers” New York.

- Awady, M. N., (1999):** Engineering of Agricultural materials processing, Memos, Col. Ag., Ain Shams U.:138p (In Arabic).
- Battisti, R. and Corrado, A. (2005):** Environmental assessment of solar thermal collectors with integrated water storage. *Journal of Cleaner Production*, 13, 1295-1300.
- Brenndorfer, B., Kennedy, L. and Mrema, G. (1987):** Solar Dryers: Their Role in Post-Harvest Processing. Commonwealth Secretariat.
- Chang, I. S. and Kim, J. H. (2001):** Development of clean technology in wafer drying processes. *Journal of Cleaner Production*, 9, 227-232.
- Chaudhari, A.D. and Salve, S.P. (2014):** A review of solar dryer technologies. *International Journal of Advancements in Technology*.
- Comsan, M. N. (2010):** Solar energy perspectives in Egypt.
- Duffie, J.A and Beckman, W. A. (1991):** Solar engineering of thermal processes. New York: Wiley.
- Edjekumhene, I. and Atakora, S.B. (2001):** Implementation of renewable energy resources – opportunities and barriers, Ghana Country Study, 48.
- Ekechukwu, O. V., & Norton, B. (1999):** Review of solar-energy drying systems II: an overview of solar drying technology. *Energy conversion and management*, 40(6), 615-655.
- Forson, F. K., Nazha, M. A. A., Akuffo, F. O. and Rajakaruna, H. (2007):** Design of mixed-mode natural convection solar crop dryers: Application of principles and rules of thumb. *Renewable Energy*, Volume 32: 2306–2319.
- Ghani, S. T., Abdel Wahed, M. S. and Jwar, A .S. (2021):** Study the effect of foliar spraying with Dionyfer and Azomin on the vegetative growth indicators of the leaves of Henna plant (*Lawsonia inermis L.*). *University of Thi-Qar Journal of agricultural research*. Volume 10, Issue 1: PP 70 – 78.
- Kalogirou, S. A. (2004):** Solar thermal collectors and applications. *Progress in Energy and Combustion Science*, 30 (2004):231-295.
- Lamidi, R. O., Jiang, L., Pathare, P. B., Wang, Y.D. and Roskilly, A.P. (2019):** Recent advances in sustainable drying of agricultural produce: A review. *Applied Energy* 233–234, 367–385. <https://doi.org/10.1016/j.apenergy.2018.10.044>.
- Mohanraj, M. and Chandrasekar, P. (2009):** Performance of a Forced Convection Solar Dryer Integrated with Gravel as Heat Storage Material for Chili Drying. *Journal of Engineering Science and Technology* 4(3): 305-314.
- Moumni, N., Youcef-Ali, S., Moumni, A. and Desmons, J. Y. (2004):** Energy analysis of a solar air collector with rows of fins. *Renewable Energy*, 29(13), 2053-2064.
- Musembi, M. N., Kiptoo, K. S. and Yuichi, N. (2016):** Design and Analysis of Solar Dryer for Mid-Latitude Region. *Energy Procedia* 100, 98 – 110.

- Perlin, J. (1999):** “From Space to Earth”, Aatec Publications, Ann Arbor, Michigan.
- Rehmat, S., Khera, R. A., Hanif, M. A., Ayub, M. A., & Hussain, A. I. (2020):** Henna. In *Medicinal Plants of South Asia* (pp. 355-368).
- Sengar, S. H., Burbade, R. G., Divyesh, V. and Abhishek, P. (2018):** Evaluation of solar tunnel dryer for green leaves drying. *Journal of Postharvest Technology*. 06(2): 38-48.
- Simon, J.E., Chadwick, A.F. and Craker, L.E.(1984):** The Scientific literature on selected herbs and aromatic and medicinal plant of the Temperate Zone, Archon Books.770 p.
- Tiwari, S., Tiwari, G.N. and Al-Helal, I.M. (2016):** Development and recent trends in greenhouse dryer: a review. *Renewable and Sustainable Energy Reviews*. 65:1048e64.
- Tonui, K.S, Mutai, E.B.K., Mutuli, D.A, Mbugu, O.O. and Too K.V. (2014):** Design and Evaluation of Solar Grain Dryer with a Backup Heater. *Research Journal of Applied Science, Engineering and Technology*. 7 (15): 3036-3043.